assuming infinite conductivity for the medium and a 45° westward shift of the equatorial magnetic field, the earth's rotation velocity would be reduced from its present value to zero in a time much smaller than the lifetime of the earth.

The classical longitude effect for cosmic-ray intensity also displays a westward shift.[2,15] We wish only to mention here that the explanation to account for the longitude shift proposed by Lemaitre,[16] namely a parallactic effect on the cosmic-ray particle trajectories, cannot account for the observed cosmic-ray equator and, indeed, is too small an effect to account for the observed longitude effect.

The distortions of the earth's outer field in the interplanetary medium and the possible existence of an outer ring current make it unlikely that the charged particles experience the field distribution of a perfect magnetic dipole. Therefore, further measurements at many longitudes are required before we can consider our representation of the effective cosmic-ray equator by a sine curve as a reasonably good approximation. We do not at present know the difficulties which may be encountered by extrapolating to high magnetic latitudes these equatorial results; preliminary measurements in the Arctic and Antarctic indicate that serious difficulties may arise.[2] However, it appears unlikely that the main features of this striking discrepancy at low latitudes will be appreciably different from those in Fig. 3.

[15] H. Hoerlin, Z. Physik **102**, 666 (1936).
[16] G. Lemaitre, Nature **140**, 23 (1937).

ACKNOWLEDGMENTS

We wish to express our gratitude to the Captain of the *U.S.S. ATKA*, Commander Glen Jacobsen, his officers and crew, and to Mr. Hugh Odishaw and the U. S. National Committee for the International Geophysical Year for making possible this joint expedition. Both Air Force and Navy groups have provided excellent assistance. We thank the University of Minnesota Cosmic Ray Group for permission to use Fig. 7. We especially thank Mrs. M. Baker, Mr. G. Lentz, Mr. J. Ayers, and Mr. Neil Sullivan of the Institute cosmic-ray group for the preparation of the data.

PHYSICAL REVIEW VOLUME 102, NUMBER 6 JUNE 15, 1956

Bubble Counting for the Determination of the Velocities of Charged Particles in Bubble Chambers*

DONALD A. GLASER, *Harrison M. Randall Laboratory of Physics, University of Michigan, Ann Arbor, Michigan*
DAVID C. RAHM, *Brookhaven National Laboratory, Upton, New York*

AND

CYRIL DODD,† *Physics Department, University College, London, England*

(Received February 23, 1956)

The density of bubbles along tracks in a liquid propane bubble chamber has been measured as a function of particle velocity for positive pions and protons with velocities $\beta=v/c>0.4$. For temperatures from 55°C to 59.5°C the bubble density, b, is described by $b=(A/\beta^2)+B(T)$, where $A=9.2\pm0.2$ bubbles/cm and B is a function of temperature only. Velocities can be determined by bubble counting, using fast comparison tracks of known velocity, with a final average error in velocity of 5% for proton tracks 10 cm long. Accurate temperature control is not required to obtain this accuracy by using this method.

I. INTRODUCTION

An important feature of the cloud chamber and nuclear emulsion for interpretation of nuclear processes is their ability to furnish information concerning particle velocities by measurement of the relative ionization. Together with other data, this ionization measurement permits the identification of particles, the determination of particle masses, and the calculation of characteristics of nuclear events.

The usefulness of the bubble chamber as a research instrument in nuclear physics is similarly much enhanced by the experimental finding that the density of bubbles along a track is a quantitative measure of the velocity of charged particles. Previously published bubble chamber photographs demonstrated this possibility qualitatively,[1] but now we have completed a systematic series of measurements which establishes the quantitative reliability of bubble counting as a technique analogous to grain counting in a nuclear emulsion or droplet counting in a cloud chamber. The bubble density measured in propane did not turn out to be proportional to the relative ionization, but rather is a linear function of $1/\beta^2$, where $\beta=v/c$ is the relativistic velocity of the particle. This result makes

* This work was supported in part by the National Science Foundation and the U. S. Atomic Energy Commission.
† Fulbright Research Scholar, University of Michigan, Fall, 1955.

[1] D. A. Glaser and D. C. Rahm, Phys. Rev. **97**, 474 (1955).

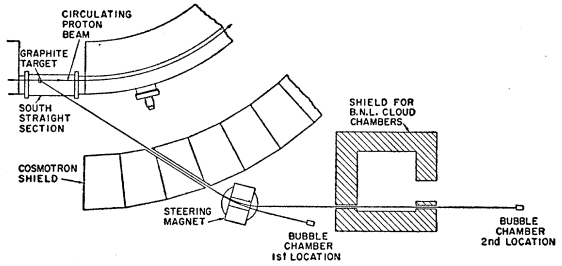

FIG. 1. Experimental arrangement (schematic). From the particles produced by the 3-Bev circulating proton beam on striking the graphite target, positive pions and protons in the momentum range 530 Mev/c to 1600 Mev/c are selected. At the first bubble chamber location, 11 feet from the steering magnet, the total spread in momentum is about 6%; at the second location, 42 feet away from the steering magnet, the spread is about 3%.

it seem likely that some of the bubbles are produced by low-energy delta rays along the track, since their number is proportional to $1/\beta^2$. All of the bubbles observed in these experiments cannot be explained so simply. A complete explanation of the observed bubble densities will probably require a detailed study of the properties of superheated liquids.

II. EXPERIMENTAL METHOD

To establish the relationship between the velocity of a singly charged particle and the density of bubbles along its track, we took photographs of a beam consisting mainly of protons and positive pions passing through the Michigan six-inch bubble chamber[1,2] filled with liquid propane. This beam was produced by the Brookhaven Cosmotron by allowing the internal 3-Bev proton beam to strike a graphite target. Particles emerging at an angle of 32° with respect to the circulating proton beam were allowed to pass through an opening in the concrete shielding wall, a gap in an exterior steering magnet, and finally the bubble chamber. By adjusting the current in the steering magnet, particles of any chosen momentum could be made to pass through the bubble chamber. A schematic diagram of the experimental arrangement is shown in Fig. 1. The bubble chamber was originally placed about 11 feet from the center of the magnet and the beam was deflected through an angle of about 19° with a maximum momentum of 1.6 Bev/c. When analysis of some of the early pictures indicated that the momentum resolution was not as good as was needed, the bubble chamber was moved to a position about 42 feet from the center of the magnet and the beam was deflected through an angle of about 32° with a maximum momentum of 915 Mev/c.

Absolute momentum calibration was done by the hot wire method with an error of less than 2%. During the later runs the magnet current was held constant within $\frac{1}{2}$%. The momentum resolution due to the width of the channels that defined the beam is estimated to have been about 6% for the first position and 2% for the second position. Scattering due to the long air path in the second location would add another 1% error for low-momentum particles. Scattering from collimator walls and magnet pole tips would contribute a few particles with widely varying momenta, but selection of parallel particles in the bubble chamber eliminated most of these.

Since the sensitive time of the six-inch bubble chamber is only 2 to 3 milliseconds, it is important that the particles arrive during this rather narrow time interval. The Cosmotron output beam has a duration of about 3 milliseconds with a time uncertainty of one millisecond with respect to its master timing system. Since the main part of the beam comes out in one millisecond, it was possible to guarantee catching a sufficient number of particles by flashing the lights for photographing the chamber just after the maximum beam intensity occurred, using a scintillation counter telescope to monitor the beam. This procedure assured us of getting substantial numbers of particles traversing the chamber during the period of uniform sensitivity. Particles arriving at other times will have anomalously low bubble densities as will be discussed below. For the best results using bubble chambers with large accelerators, it is therefore desirable to have beam pulses of very short duration.

Some difficulty was experienced in maintaining the temperature of the chamber constant, because the mechanical work done on the liquid during recompression added a few watts of heat to the liquid during extended runs. Temperatures were maintained stable to about 0.1°C during each run at a given momentum, though the thermistor-controlled oven temperature was more closely controlled. Also the temperature uniformity across the chamber was much better than 0.1°C. By compensating for this source of heat it has since been possible to achieve much better temperature control.[2]

Each picture contained up to 20 countable tracks, some of which were minimum-ionizing pions and some protons ionizing more heavily. Their momenta ranged from 530 Mev/c to 1.6 Bev/c. Some minimum-ionizing tracks appeared in practically every picture so that we could check ratios of bubble densities against relative ionizations and velocities as well as the absolute values of these quantities. The bubble densities were measured for tracks having different rates of energy loss ranging from the minimum value up to about four times minimum. Most of the measurements in propane were made at 55.5°C, 56.5°C, 57.5°C, and 59.5°C, although a few measurements were made at 50°C, 52°C, 53°C, 54°C, and 55°C.

III. MEASUREMENTS AND CORRECTIONS

Measurements were made by aligning the image of a track on the negative with the precision motion of a

[2] D. C. Rahm, Ph.D. thesis, University of Michigan, 1956 (unpublished).

traveling microscope and counting the bubbles as their images were moved slowly across the center of the field of view. Bubble densities up to about 150 bubbles per centimeter on the negative could be counted with negligible error due to fusion of neighboring bubble images. Since the average photographic demagnification was 2.5, this corresponds to 60 bubbles per centimeter on the original track. This limitation is essentially optical, arising from the fact that the smallest bubble images on the negative are 40 microns in diameter as a result of diffraction and depth of field effects.

Only those tracks which were found by stereoscopic inspection to be closely parallel to the expected beam direction were accepted for measurement. In this way most of the particles scattered by the collimators and chamber walls were eliminated from consideration. In addition, the true lengths of the measured track segments were obtained by making a correction for the variation of magnification with depth. This correction amounted to about 3% in the final bubble densities.

The most important correction by far arises from the fact that each photograph contains tracks of various ages because the beam pulse is several milliseconds long. A number of tracks were found to have fewer bubbles than expected even for minimum ionizing particles. Since these tracks always consisted of abnormally large bubbles, it was concluded that they were old tracks formed during the early phase of the expansion of the chamber before it was fully sensitive. The existence of such a phase of incomplete sensitivity has already been established experimentally.[1,2] By eliminating all tracks whose bubble images were larger than 0.100 mm in diameter, all the "subminimum" tracks were eliminated and the histograms displaying the results became much more sharply peaked. The choice of the largest admissible bubble size which gives reliable bubble counts depends on the relative timing of the beam pulse and the lights and slightly on the temperature. This limiting size can be determined easily for a given experimental arrangement by counting bubbles on a few minimum-ionizing tracks of various bubble sizes.

Finally, the incident energy of the particles was corrected for the energy loss in the walls of the oven and the chamber, and for half the loss in the propane. The small error made by averaging the bubble density over the whole track of a particle which is slowing down slightly, is not serious in most of the cases considered in detail here. For the few cases of stopping particles which were measured, bubbles were counted for only a small portion of the total visible track length.

IV. RESULTS

When straight parallel beam tracks of small bubbles are selected and the measured bubble densities corrected as described in the last section, the resulting bubble densities corresponding to a single momentum value fall into two main groups as shown by the typical histogram in Fig. 2. Pion tracks of initial momentum 915 Mev/c contain about 200 bubbles and proton tracks of the same momentum contain about 340 bubbles for tracks about 12.5 centimeters long at 55.5°C. Assuming the bubbles to result from statistically independent events, the corresponding errors resulting from fluctuations in the total number of bubbles on a track are 7% and 5.4% for a single track of this length. From the final form of the relationship between bubble density and particle velocity, we conclude that the spread in momentum of the particles used for this measurement contributes as much as 3% error in bubble density for the slower particles, and not at all for the fastest.

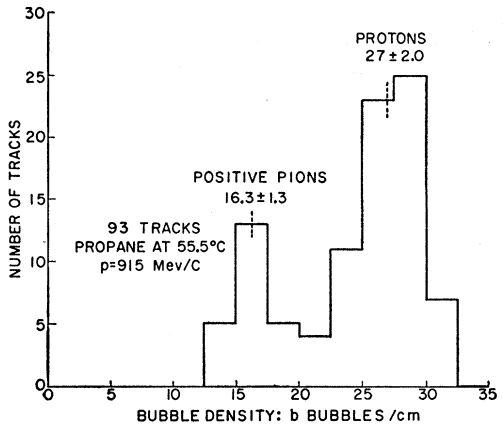

FIG. 2. Histogram showing the relative frequency of measured corrected bubble densities. The incident beam contained protons and positive pions of momentum 915±30 Mev/c. The liquid is propane at 55.5°C. In the propane the relativistic velocities are $\beta=0.676$ for the protons and $\beta=0.988$ for the pions. The protons are losing energy at 1.64 times the minimum energy loss.

The resulting error of 8 or 9% is consistent with the width of the peaks in Fig. 2, so we can expect the accuracy of our measurements on single unknown tracks to be limited mainly by the statistical fluctuations in the number of bubbles formed, counting errors being negligible. For bubble densities exceeding 60 bubbles per centimeter, however, fusion of neighboring bubbles, or, more likely, bubble images, begins to limit the counting accuracy. Since all of the images are along the line of the track, and not diffused as are droplet images on cloud chamber tracks, photoelectric bubble counting may be possible. To investigate its feasibility we have made microphotometer traces of the negatives for tracks of various bubble sizes and densities. The results make it seem promising to try photoelectric bubble counting. Aside from the obvious labor-saving advantages, an automatic method might make possible some reproducible way of counting fused and almost fused images so that a reliable empirical calibration can be established, even if each individual bubble is not counted. Human observers vary in their judgment of

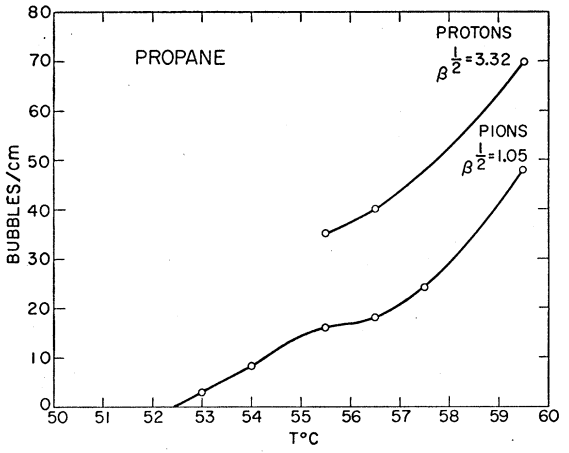

FIG. 3. Observed bubble density in propane *versus* temperature for pions with $1/\beta^2=1.05$ and protons with $1/\beta^2=3.32$. The total track lengths measured are sufficient to reduce statistical errors below 2% in bubble density. The momentum spread in the proton beams contribute an error of about 3% in bubble density.

fused images and give an unreproducible error in counting dense tracks.

The measured bubble densities are found to depend rather sharply on the temperature, as shown in Fig. 3. From these curves one can estimate the temperature stability required to maintain a given maximum error in bubble density. In propane at 56°C, temperature stability of about 0.1°C is needed to hold the bubble density constant within 2% for $1/\beta^2$ lying between 1 and 3.3.

From measurements of the thermodynamic conditions required for bubble nucleation in several liquids exposed to various radiations,[3] and from theoretical ideas concerning the microscopic mechanism of the process,[4] we have concluded that bubbles are nucleated along the path of a charged particle by local deposit of energy in the liquid by delta rays. We therefore did not expect to find that the bubble density is proportional to the relative ionization of the particle, but rather that it depends on the delta-ray density. Figure 4 shows that the bubble density is not a linear function of relative ionization, especially at large values of the ionization.

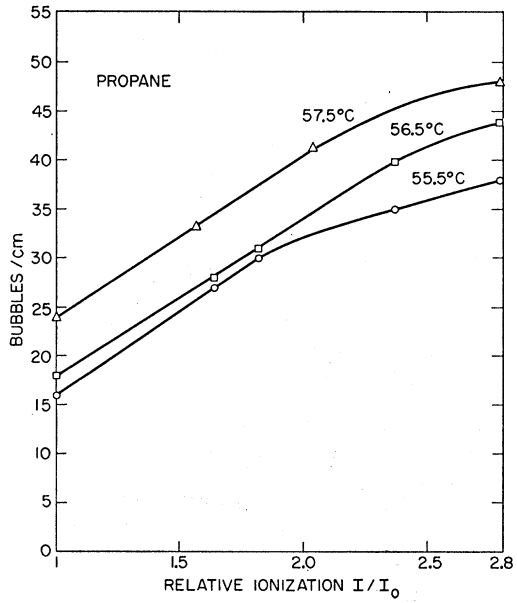

FIG. 4. Observed bubble density in propane *versus* relative ionization for three temperatures. The bubble density is not linear with relative ionization. Errors are less than 5% in bubble density except for possible temperature variations between runs.

The number of delta rays in a given energy range produced by a charged particle flying through the liquid can be calculated by integrating the collision cross section for the moving particle against free electrons over the chosen range of energies of the ejected electrons. Using known cross sections,[5] one finds that relativistic terms and terms dependent on particle spin contribute less than 1% for the cases of interest here. The resulting number of delta rays whose energies lie between E_1' and E_2' electron volts is

$$n_\delta=\frac{1.53\times10^5 Z/A}{\beta^2}\left[\frac{1}{E_1'}-\frac{1}{E_2'}\right]\text{g}^{-1}\text{ cm}^2, \qquad (1)$$

where Z and A are the charge and mass numbers of the liquid and $\beta=v/c$ for the particle. This formula is valid only when the lower energy limit, E_1' is at least three times the average ionization potential of the atoms of the liquid, for only in that case can the atomic binding energy of the electrons be neglected as was done in deriving Eq. (1). In comparing n_δ with the bubble density, we include only those bubbles which lie on the track, and exclude those belonging to a very energetic delta ray that extends some distance away from the track. This procedure leads to an upper limit, $E_2'\approx50$ kev. Since E_1' is only a few kev, n_δ is not very sensitive to the exact value of E_2'. If we suppose that all delta rays more energetic than E_1' are able to nucleate a bubble, we expect the bubble density to be proportional to $1/\beta^2$. If we further suppose that changing the temperature changes the threshold delta-ray energy required for bubble nucleation, we expect the bubble density, b, to obey to relationship

$$b=C(T)/\beta^2 \text{ bubbles/cm}, \qquad (2)$$

where $C(T)$ is a function of the temperature, T, through E_1' and because of the variation of the density of the liquid with temperature.

In Fig. 5 we see that the bubble density is indeed a linear function of $1/\beta^2$, although the scatter of points is worse than expected from statistical fluctuations and momentum spread in the beam. The data do not fit Eq. (2), however, but are fairly well represented by a

[3] D. A. Glaser and L. O. Roellig (to be published).
[4] D. A. Glaser (to be published).
[5] B. Rossi, *High-Energy Particles* (Prentice-Hall Inc., New York, 1952), p. 15.

family of parallel lines described by

$$b=(A/\beta^2)+B(T) \text{ bubbles/cm} \quad (3)$$

in which only B is temperature-dependent and the slope, A, seems roughly independent of temperature. Since temperature instability was one of the main difficulties in carrying out these measurements because of the extra heat of recompression described above, we believe that some of the scatter of points in Fig. 5 is due to temperature variations. During a run at a given momentum the temperature could not have changed much, but from one run to the next at a different momentum, the temperature might have changed.

To reduce this uncertainty due to temperature fluctuations, one can use the tracks of fast particles present in every picture as comparison tracks. This is similar to the use of minimum ionization tracks for standardization and calibration of ionization measure-

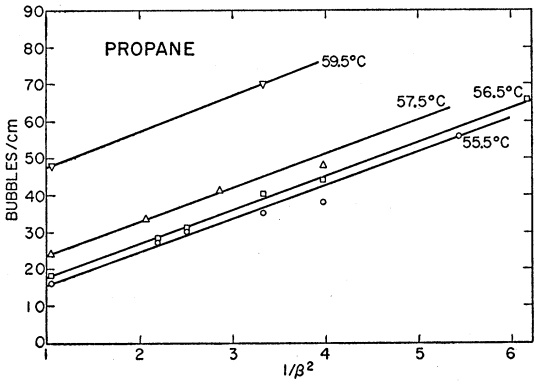

FIG. 5. Observed bubble density in propane *versus* $1/\beta^2$ for the moving particles. Lines of constant slope fit the data roughly. The scatter of points is probably due to temperature variations between runs. Other errors are less than 5% in bubble density.

ments in cloud chambers and nuclear emulsions. In the case of bubble counting we notice that using Eq. (3) we can form temperature-independent differences,

$$b_1-b_2=A(1/\beta_1^2-1/\beta_2^2) \text{ bubbles/cm}, \quad (4)$$

by subtracting the bubble counts of two different tracks in the same picture or run, for which the temperatures are the same. Choosing the fast pions with $\beta\approx 1$ as comparison particles we can plot the bubble density differences according to Eq. (4). This has been done in Fig. 6 in which all the bubble density data taken at 55.5°C, 56.5°C, 57.5°C, and 59.5°C reduce quite remarkably to a single universal curve. From Fig. 6 we find that $A=9.2\pm 0.2$ bubbles/cm for protons in propane. Preliminary measurements at 55°C are consistent with this same value of A, but measurements at 54°C, 53°C, and 52°C, indicate that A becomes smaller below 55°C. At 50°C no tracks are visible, at 52°C only stopping protons can be seen, and at 53°C

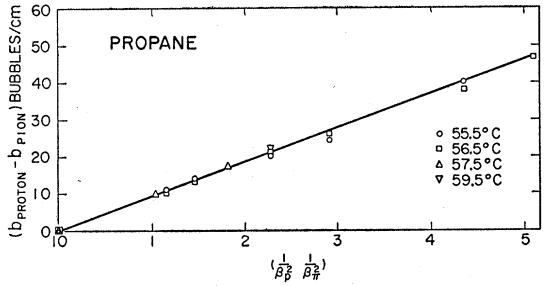

FIG. 6. All the observed densities are reduced to a single straight line by using fast minimum ionizing pions as comparison tracks. This minimizes errors due to temperature fluctuations and provides a temperature-independent means of measuring particle velocities. Errors due to momentum spread in the beam may be 5% for the slower particles.

and 54°C, minimum ionizing pions made 2.9 bubbles/cm and 8.1 bubbles/cm respectively as shown in Fig. 3. Our measurements indicate, therefore, that Eq. (4) is valid with constant A for propane from 55°C to 59.5°C and for values of $1/\beta^2$ up to about 6. The variation of $B(T)$ with temperature is shown in Fig. 7. If Eq. (4) is found to describe the bubble density at temperatures below 55°C, A will be less than 9.2 bubbles/cm.

The explanation of the empirical result expressed by Eq. (3) must certainly depend on the microscopic mechanism of bubble nucleation by ionizing events. It will involve properties of the liquid and details of the process by which charged particles lose energy in penetrating the liquid. One therefore expects that the values of A and $B(T)$ as well as the range of validity of Eq. (3) will be different for different liquids. It is important for the interpretation of bubble chamber

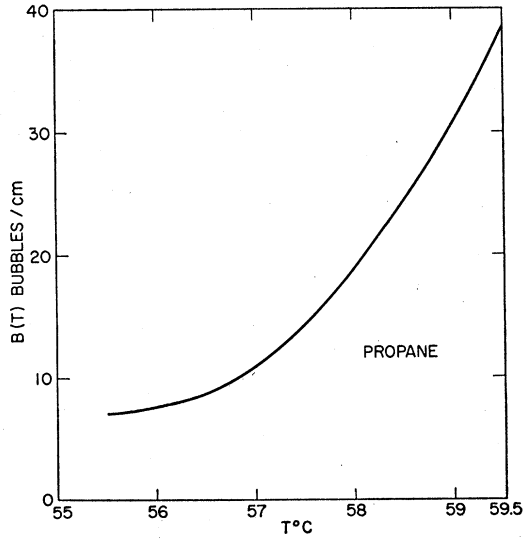

FIG. 7. Temperature-dependent part of the observed bubble density in propane, $B(T)=b-(9.2/\beta^2)$ bubbles/cm plotted *versus* temperature. $B(T)$ does not depend on the velocity of the particle making the track.

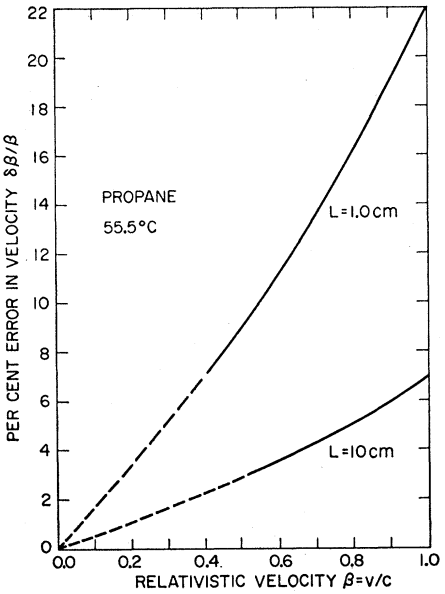

FIG. 8. Percent errors in determining charged particle velocities by bubble counting are plotted *versus* particle velocity for propane. Only statistical fluctuations in bubble production are considered in these estimates, shown for 1-cm and 10-cm track segments. These errors do not apply to slow particles because the bubble density varies along the segment counted. The solid parts of the curves show the approximate region of validity for protons.

photographs to know if these numerical results apply to any propane chamber, or whether they depend on the details of the expression process and therefore apply only to the chamber used in these experiments. We have no direct evidence on this point, except that the existence of a plateau of uniform sensitivity for both the 6-inch chamber used here, and a 2-inch chamber with much different expansion hydrodynamics described previously[1] implies that conditions in the chamber, at least during this brief interval of uniform sensitivity, are not highly dependent on the details of the expansion process. Slight changes in expansion ratio which must have occurred during this experiment do not seem to have affected the results greatly either. Careful calibration with different chambers will settle this question.

V. CONCLUSIONS AND APPLICATIONS

These results suggest a procedure for using bubble counting for determining the velocities of charged particles in nuclear events photographed in bubble chambers. Provision should be made that each picture, or at least a few pictures in each run, have tracks of particles of known velocity. Since the particles will generally be selected by magnetic deflection, fast particles should be used where possible because their velocity is least sensitive to momentum errors. If a number of long calibration tracks are used, the error in the measurement of their bubble densities can be made quite small, as it is limited principally by statistics. Then Eq. (4) can be used to find the velocity β_1, of the unknown particle from its bubble density b_1. Since A, b_2, and β_2 can be measured very well as described above, the uncertainty in the unknown velocity β_1 will result mainly from the uncertainty in b_1, which is a consequence of statistical fluctuations in the production of bubbles on the unknown track. This procedure is equivalent to determining accurately the values of A and B in Eq. (3).

We calculate the percent error in β, assuming A and B to be known exactly. From Eq. (3), we find by taking the absolute value of the logarithmic derivative,

$$\frac{\delta\beta}{\beta}=\frac{1}{2}\frac{\delta(b-B)}{b-B}=\frac{1}{2}\frac{\delta b}{b-B}. \tag{5}$$

For a track of length L centimeters, the standard deviation in the total number of bubbles is $(bL)^{\frac{1}{2}}$, assuming the bubbles to be formed by random, independent events, since bL is the average total number of bubbles. Then we put $\delta b=(bL)^{\frac{1}{2}}/L$ into Eq. (5) and use Eq. (3) to find

$$\frac{\delta\beta}{\beta}=\frac{1}{2}\left(\frac{b}{L}\right)^{\frac{1}{2}}\frac{1}{b-B}=\frac{\beta}{2(AL)^{\frac{1}{2}}}\left(1+\beta^2\frac{B}{A}\right)^{\frac{1}{2}}. \tag{6}$$

We see that the percent error in the velocity varies inversely as the square root of the track length and can be reduced by lowering the temperature to make $B(T)$ smaller. Reduction of the temperature below a certain value is impractical, however, for the bubbles on lightly ionizing tracks become so sparse that the tracks are very difficult to see, and their points of intersection in nuclear collisions become uncertain. On the other hand, the bubble densities of very slow particles can be measured reliably only at fairly low temperatures. Some types of observations may therefore require high operating temperatures, while others may be possible only at low temperatures. In Fig. 8 are plotted the approximate percent errors in β calculated from Eq. (6) for propane at 55°C using 10-cm and 1.0-cm track lengths. For low velocities, shown as dotted portions of the curves, β changes considerably along the track due to the energy loss, even for protons. Measurements on the increase in bubble density along the track of a stopping particle should make it possible to use bubble density *versus* residual range as a means of estimating particle masses.

ACKNOWLEDGMENTS

We are grateful to the Cosmotron staff at Brookhaven National Laboratory for making these experiments possible, and especially to the members of the Cloud Chamber Group at the Laboratory for their extensive help in carrying out the exposures.